

General mechanism for death in coupled systems

V. Resmi* and G. Ambika†

Indian Institute of Science Education and Research, Pune - 411021, India

R. E. Amritkar‡

Physical Research Laboratory, Ahmedabad - 380009, India

We introduce a general mechanism for amplitude death in coupled dynamical systems. Two systems coupled directly can synchronize with sufficient strength of coupling. When an indirect feedback coupling through an environment or an external system is introduced in them, it is found to induce a tendency for antisynchronization. For sufficient strengths, these two competing effects can lead to amplitude death. We have analyzed in detail the nature of the transition to death. This mechanism is quite general and works for different types of systems such as periodic, chaotic and time-delay systems and for different types of direct coupling such as diffusive, substitution and synaptic couplings.

PACS numbers: 05.45.Xt

1. INTRODUCTION

The complex dynamics of many real systems can be understood as the collective behaviour of a large number of dynamical units coupled via their mutual interactions. Such connected systems has been an interesting topic of study especially due to its relevance in understanding a large variety of natural systems. Based on the the nature of interactions among the coupled units, they can exhibit many emergent phenomena such as synchronization, hysteresis, phase locking, phase shift, amplitude death and oscillator death [1–3]. Among these, the phenomenon of synchronization forms the most widely studied one and has relevance in many contexts such as neuronal networks, communication, laser systems etc [1]. So also, the quenching or suppression of dynamics called amplitude death is another emergent phenomenon of equal relevance in such systems. This can lead to interesting self adjustable control mechanisms and has a prominent role as an efficient regulator of the dynamics. The occurrence of amplitude death has been reported in various physical and biological systems such as BZ reactions [4, 5], cardiac rhythms, ecological systems, cardiac pace maker cells, coupled laser systems [6, 7], relativistic magnetrons [19]. We would like to project the importance of the phenomena of death in coupled systems both as a desirable control mechanism in cases such as coupled lasers where it leads to stabilization [20, 21] and as pathological cases of oscillation suppression or disruption in cases like neuronal disorders such as Alzheimer’s disease, Parkinson’s disease etc [8–10].

The mechanisms so far reported to induce amplitude death are detuning of oscillators under strong coupling [11, 12], coupling through conjugate variables [13] and

delay in the coupling due to finite propagation or information processing speeds [14, 24]. Distributed delays rather than discrete or constant delays have been proposed as more realistic models in ecology and neurobiology, where the variance of the delay plays a relevant role [15]. In all these mechanisms, death occurs dynamically due to the targeting of the units to one or more of the equilibrium states or due to the stabilization of one of these states. The equilibrium states or fixed points can be either that of the uncoupled system or those evolved by coupling. While these mechanisms can model the amplitude death observed in coupled systems of oscillators, we find that all these methods are system specific and may not work in a general case. Also, there are cases like neuronal disorders where depression of activity or death is due to the presence of another agency or medium [8, 9]. For such cases, the mechanism of death is still not fully understood and all the above mentioned mechanisms will not be applicable.

In this work, we introduce a mechanism for death caused by an indirect feedback coupling in addition to direct coupling. We find that while it essentially explains quenching of activity or suppression induced by an external medium or agent, this novel method can also serve as a general mechanism to induce death in coupled systems. Its generality lies in the fact that it is effective in quenching dynamics in a variety of systems such as periodic oscillators, chaotic systems and delay systems and with different forms of coupling interactions such as diffusive, synaptic etc. As such it is an important step in methodology towards achieving controls or stabilization to desirable performance in many practical cases. One of the novel features of our method is that death can be engineered and can be easily implemented in any system with coupled synchronizable units.

We have shown in an earlier work that indirect feedback coupling through environment can induce antiphase (or anti) synchronization in two systems which are not directly connected [16]. In the present work we start with two systems coupled directly such that with suffi-

*Electronic address: v.resmi@iiserpune.ac.in

†Electronic address: g.ambika@iiserpune.ac.in

‡Electronic address: amritkar@prl.res.in

cient strength of coupling, they can exhibit synchronous behaviour. When the indirect feedback coupling through the environment or another external system is introduced in them, it is found to induce tendency for antisynchronization and for sufficient strengths, these two competing effects balance to produce amplitude death. We find that then the subsystems stabilize to the same or different fixed points of the coupled system. An approximate stability analysis is given for the general context. We have analysed in detail the nature of transition to AD state from initial synchronized behaviour. Specific cases we study fall into two different types, continuous and discontinuous transitions. In the continuous case, as illustrated by two coupled Rössler systems, during the transition the full reverse period doubling scenario is observed reaching a one-cycle state before AD occurs. In the discontinuous state, for two coupled Lorenz systems, the systems go through a state of frustration between synchronized and anti-synchronized behaviour.

2. AMPLITUDE DEATH VIA DIRECT AND INDIRECT COUPLING

We start with two systems coupled mutually via diffusive coupling and indirect coupling through an environment as given by

$$\dot{x}_1 = f(x_1) + \epsilon_d \beta(x_2 - x_1) + \epsilon_i \gamma y \quad (1a)$$

$$\dot{x}_2 = f(x_2) + \epsilon_d \beta(x_1 - x_2) + \epsilon_i \gamma y \quad (1b)$$

$$\dot{y} = -\kappa y - \frac{\epsilon_i}{2} \gamma^T (x_1 + x_2) \quad (1c)$$

Here, x_1 and x_2 represent two oscillators whose intrinsic dynamics is given by $f(x_1)$ and $f(x_2)$ respectively. The environment is modeled by a one dimensional overdamped oscillator y with a damping parameter κ . The environment is kept active by feedback from both the systems as given by the last term in Eq.(1c). The systems are mutually coupled using diffusive coupling (second term in Eq.(1a & 1b)). Both the systems also get feedback from y (last term in Eq.(1a & 1b)). The components of x_i that take part in the coupling are decided by two matrices, β and γ whose elements are either zero or one. We take ϵ_d to be the strength of direct diffusive coupling between the systems, and ϵ_i be the strength of feedback coupling between the systems and environment.

We illustrate the scheme for coupled chaotic Rössler systems represented by the following equations.

$$\begin{aligned} \dot{x}_{i1} &= -x_{i2} - x_{i3} + \epsilon_d(x_{j1} - x_{i1}) + \epsilon_i y \\ \dot{x}_{i2} &= x_{i1} + a x_{i2} \\ \dot{x}_{i3} &= b + x_{i3}(x_{i1} - c) \\ \dot{y} &= -\kappa y - \frac{\epsilon_i}{2} \sum_i x_{i1} \end{aligned} \quad (2)$$

The resulting time series for synchronized state with only direct coupling and amplitude death state with both direct and indirect couplings are shown in Fig. 1. When

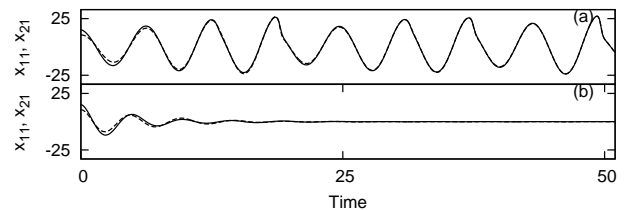


FIG. 1: Time series of the first variable x_{i1} of two coupled Rössler systems without neglecting the transients. (a) Synchronization for $(\epsilon_d, \epsilon_i) = (0.2, 0.0)$. (b) Amplitude death for $(\epsilon_d, \epsilon_i) = (0.2, 1.0)$. Here, the Rössler parameters are $a = b = 0.1$, $c = 18$.

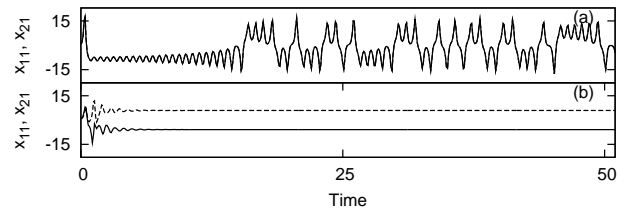


FIG. 2: Time series of the first variable x_{i1} of the coupled Lorenz system for the parameters $(\sigma = 10, r = 28, b = 8/3)$. (a) Synchronization for $(\epsilon_d, \epsilon_i) = (5, 0)$. (b) Amplitude death for $(\epsilon_d, \epsilon_i) = (5, 12)$. Here, the transients are not neglected.

$\epsilon_i = 0$, and ϵ_d is sufficiently large, we observe synchronization (Fig. 1(a)). When ϵ_i is increased, the systems stabilize to a state of amplitude death (Fig. 1(b)).

The same scheme is applied to two coupled chaotic Lorenz systems as given by the following equations.

$$\begin{aligned} \dot{x}_{i1} &= \sigma(x_{i2} - x_{i1}) + \epsilon_d(x_{j1} - x_{i1}) + \epsilon_i y \\ \dot{x}_{i2} &= (r - x_{i3})x_{i1} - x_{i2} \\ \dot{x}_{i3} &= x_{i1}x_{i2} - b x_{i3} \\ \dot{y} &= -\kappa y - \frac{\epsilon_i}{2} \sum_i x_{i1} \end{aligned} \quad (3)$$

We find that amplitude death is possible in this case also. This is shown in Fig. 2, where time series for a synchronized state (Fig. 2(a)) and an amplitude death state (Fig. 2(b)) are shown.

3. LINEAR STABILITY ANALYSIS

We analyze the stability of the steady state of two systems coupled via the scheme given in Eq.(1). For this, the variational equations formed by linearizing Eq.(1) are written as

$$\begin{aligned} \dot{\xi}_1 &= f'(x_1)\xi_1 + \epsilon_d \beta(\xi_2 - \xi_1) + \epsilon_i \gamma z \\ \dot{\xi}_2 &= f'(x_2)\xi_2 + \epsilon_d \beta(\xi_1 - \xi_2) + \epsilon_i \gamma z \\ \dot{z} &= -\kappa z - \frac{\epsilon_i}{2} \gamma^T (\xi_1 + \xi_2) \end{aligned} \quad (4)$$

We denote synchronizing and anti-synchronizing tendencies through variables ξ_s and ξ_a respectively as given

by

$$\begin{aligned}\xi_s &= \xi_1 - \xi_2 \\ \xi_a &= \xi_2 + \xi_2\end{aligned}\quad (5)$$

Then Eq.(4) can be written as

$$\begin{aligned}\dot{\xi}_s &= f'(x_1)\xi_1 - f'(x_2)\xi_2 - 2\epsilon_d\beta\xi_s \\ \dot{\xi}_a &= f'(x_1)\xi_1 + f'(x_2)\xi_2 + 2\epsilon_i\gamma z \\ \dot{z} &= -\kappa z - \frac{\epsilon_i}{2}\gamma^T\xi_a\end{aligned}\quad (6)$$

For stability, all the Lyapunov exponents obtained from Eq. 6 should be negative. Assuming that the time average values of $f'(x_1)$ and $f'(x_2)$ can be replaced by an effective μ , and ξ_1 and ξ_2 are scalars as an approximation Eq.(4) is

$$\dot{\xi}_s = \mu\xi_s - 2\epsilon_d\xi_s \quad (7a)$$

$$\dot{\xi}_a = \mu\xi_a + 2\epsilon_i z \quad (7b)$$

$$\dot{z} = -\kappa z - \frac{\epsilon_i}{2}\xi_a \quad (7c)$$

We note that Eq.(7b & 7c) are coupled while Eq. (7a) is independent of the other two. Hence, the condition for synchronized state to be stable is given by (from 7a)

$$\epsilon_d > \frac{\mu}{2} \quad (8)$$

The condition for stability of the anti-synchronized state is obtained by evaluating the eigen values λ , of the Jacobian (from 7b & 7c)

$$J = \begin{pmatrix} \mu & 2\epsilon_i \\ -\epsilon_i/2 & -\kappa \end{pmatrix}$$

Then,

$$\lambda = \frac{(\mu - \kappa) \pm \sqrt{(\mu - \kappa)^2 - 4(\epsilon_i^2 - \mu\kappa)}}{2} \quad (9)$$

$\text{Re}[\lambda]$ to be negative for both the solutions, the stability criteria is given by

1. If $(\mu - \kappa)^2 < 4(\epsilon_i^2 - \mu\kappa)$, λ is complex and the condition of stability is

$$\kappa > \mu \quad (10)$$

2. If $(\mu - \kappa)^2 > 4(\epsilon_i^2 - \mu\kappa)$, λ is real and the stability condition becomes $\kappa > \mu$ and

$$\epsilon_i^2 > \mu\kappa \quad (11)$$

Thus, Eq.(8) is the condition for stability of synchronized state which is independent from Eq. (10 & 11), which are conditions for the stability of anti-synchronized state. If Eq. (8,10 & 11) are simultaneously satisfied, the oscillations can not occur and the systems stabilize to a

steady state of amplitude death. For a given κ and μ , the transitions to amplitude death occurs at critical coupling strengths ϵ_{ic} and ϵ_{dc} independent of each other. That is

$$\epsilon_{dc} = \text{const} \quad (12)$$

and

$$\epsilon_{ic} = \text{const} \quad (13)$$

These stability criteria are numerically verified for a specific case in the following section.

4. NUMERICAL ANALYSIS

The scheme of coupling introduced in Eq. 1 is applied to the case of two Rössler chaotic systems and numerically analyzed for specific values of parameters. When coupling through the environment is absent ($\epsilon_i = 0$) and for sufficiently large strengths of direct coupling the systems are synchronized (Fig. 1(a)). With increasing ϵ_i , the systems stabilize to steady states (Fig. 1(b)). The occurrence of AD is confirmed by calculating the Lyapunov exponents [17] also. When the systems are in AD state, all the Lyapunov exponents of the coupled system are found to be negative.

This transition is studied by identifying regions of amplitude death in the parameter plane of coupling strengths ($\epsilon_i - \epsilon_d$) for a chosen value of κ . To characterize amplitude death state, we use the average amplitude of the oscillators as the index. The amplitude of the oscillators, A is taken to be the difference between the maximum and minimum values of x_1 over sufficiently long period of time. The parameter at which A becomes 0 is identified as the threshold values for onset of stability of amplitude death states. This is shown in Fig. 3. The points obtained from numerical simulations agree with the stability criteria (12 & 13) obtained in the previous section.

We also verify numerically the criteria for transition to AD given in (Eq. 11). For this the numerically obtained values of ϵ_{ic}^2 is plotted against κ and is shown in Fig. 4. The line correspond to the stability condition (Eq. 11) and the points are obtained from numerical simulations. It is seen that the agreement is good for higher values of κ . However, for low values of κ , the points deviate from straight line behaviour. We attribute this to the approximations used in the stability analysis.

4.1. Coupled Rössler systems

Further, we present the complete phase diagram in the parameter plane of coupling strengths identifying the regions of different dynamic states such as amplitude death, complete synchronization and antisynchronization. Amplitude death states are identified using A

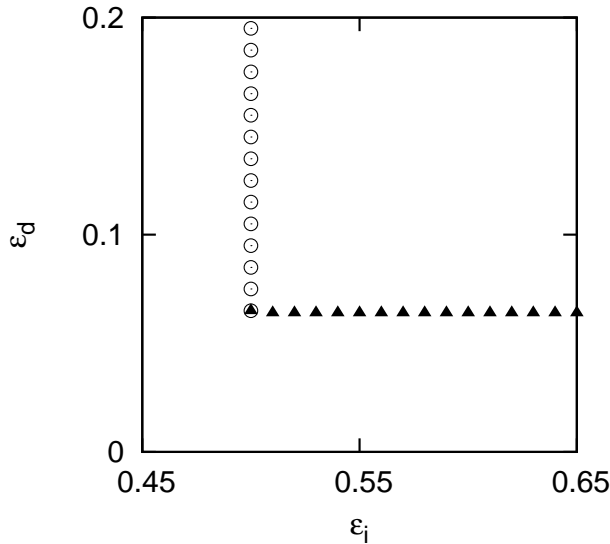


FIG. 3: Transition from regions of oscillations to amplitude death is shown in the parameter plane $\epsilon_i - \epsilon_d$ for the coupled Rössler systems. Numerical simulations are done with $\kappa = 1$. The coupling strength ϵ_d is varied from 0.0 to 0.2 in steps of 0.001. For each value of ϵ_d , ϵ_i is increased in steps of 0.001 in the range 0.45 to 0.65. The points mark the parameter values $(\epsilon_{ic}, \epsilon_{dc})$ at which the transition to AD occurs. Solid triangles agree with stability condition Eq.12 and circles corresponds to stability condition Eq.13.

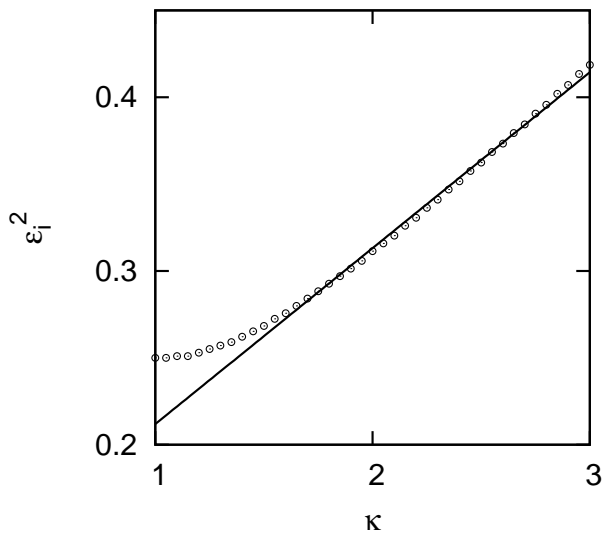


FIG. 4: Transition from regions of oscillations to amplitude death is shown in the parameter plane $\kappa - \epsilon_i^2$ for the coupled Rössler systems. The points are obtained numerically when the average amplitude becomes zero. Solid curve is a linear fit corresponding to the stability condition Eq.11, with the effective $\mu = 0.1$. The deviation from straight line behaviour for low values of κ is due to the approximations used in the stability analysis.

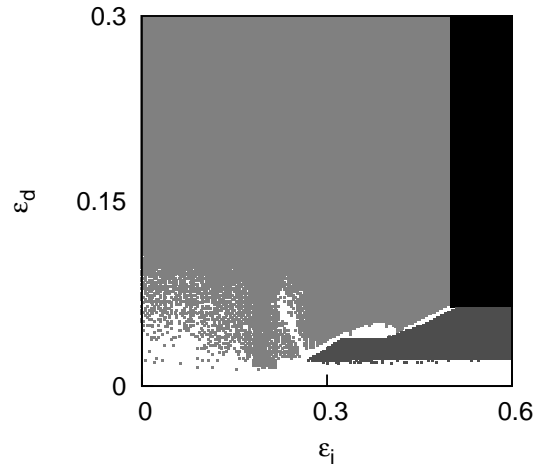


FIG. 5: Regions of different dynamical states in the parameter plane of coupling strengths $(\epsilon_i - \epsilon_d)$ in the case of two coupled Rössler systems. The indices used to identify the different regions are correlation and range. Black region corresponds to states of amplitude death ($R \sim 0$), light grey region corresponds to synchronized states ($C \sim 1$), dark grey region correspond to anti-synchronized states ($C \sim -1$) and white region correspond to desynchronized states.

as mentioned above. To identify synchronized or anti-synchronized states we use asymptotic correlation value as the index, calculated using the following equation

$$C = \frac{(x_1(t) - \langle x_1(t) \rangle)(x_2(t) - \langle x_2(t) \rangle)}{\sqrt{(x_1(t) - \langle x_1(t) \rangle)^2 (x_2(t) - \langle x_2(t) \rangle)^2}} \quad (14)$$

The phase diagram thus obtained for the coupled Rössler system is shown in Fig. 5. When the coupling strengths ϵ_d and ϵ_i are small, the systems are not synchronized (white regions in Fig. 5). For small values of ϵ_i , when ϵ_d is increased, the systems synchronize (light-grey regions in Fig. 5). When ϵ_i is increased, the systems become antisynchronized (light-grey regions in Fig. 5). When both the coupling strengths are above a certain threshold as given by the stability conditions Eq. 8 and Eq. 11, the systems stabilize to the state of amplitude death (black regions in Fig. 5).

The nature of the transitions to the state of amplitude death is further characterized by fixing one of the parameters ϵ_i or ϵ_d and varying the other. This is shown in Fig. 6. Here, the transition from oscillatory state to amplitude death state is continuous such that as the coupling strength is increased, the amplitude of the oscillations gradually decreases to zero. We also notice from the time series and phase space plot that as the coupling strength (ϵ_d or ϵ_i) increases, the Rössler systems undergo the full reverse period doubling sequence to one-cycle and then goes to AD state. The bifurcation diagram for this transition is shown in Fig. 7. A similar type of transition from chaotic state to AD state via a limit cycle in the case of Rössler systems with delay in coupling has been

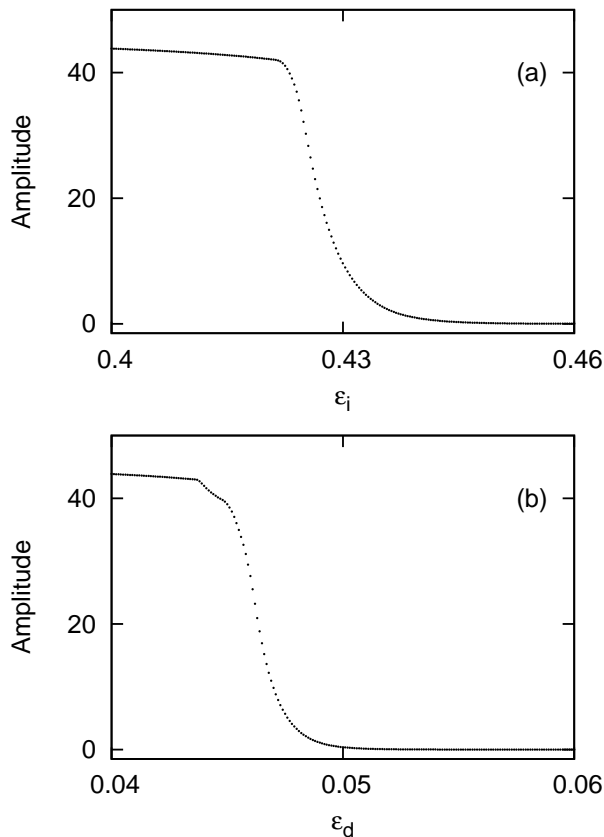


FIG. 6: Transition to state of amplitude death for coupled Rössler systems. Here, the strength of one coupling is kept fixed, while varying the other. (a) varying ϵ_i while keeping $\epsilon_d = 0.2$ (b) varying ϵ_d while keeping $\epsilon_i = 0.5$. In both cases, the transitions are continuous.

previously reported in [24]. But in our case, we could observe in this transition, the full period doubling scenario in the reverse direction.

4.2. Coupled Lorenz systems

The same study is repeated in the case of two coupled Lorenz systems. It is interesting to note that in this case, the two systems stabilize to two different fix points (Fig. 2(b)). The regions of different dynamical states in the parameter plane of coupling strengths in the case of Lorenz systems is shown in Fig. 8. When both ϵ_d and ϵ_i are low, the systems are not synchronized (white region). For very small values of ϵ_d and large ϵ_i , the systems are antisynchronized (dark-grey), and when ϵ_d is increased, the systems are in AD state (black region). For small values of ϵ_i and large ϵ_d , the systems are synchronized (light-grey). As ϵ_i increases, the systems first lose synchronization (Fig. 9). In Fig. 9, time series of the synchronization error between the two Lorenz systems is shown. For higher values of ϵ_i , they stabilize to the state of AD (black). In the desynchronized state before the AD

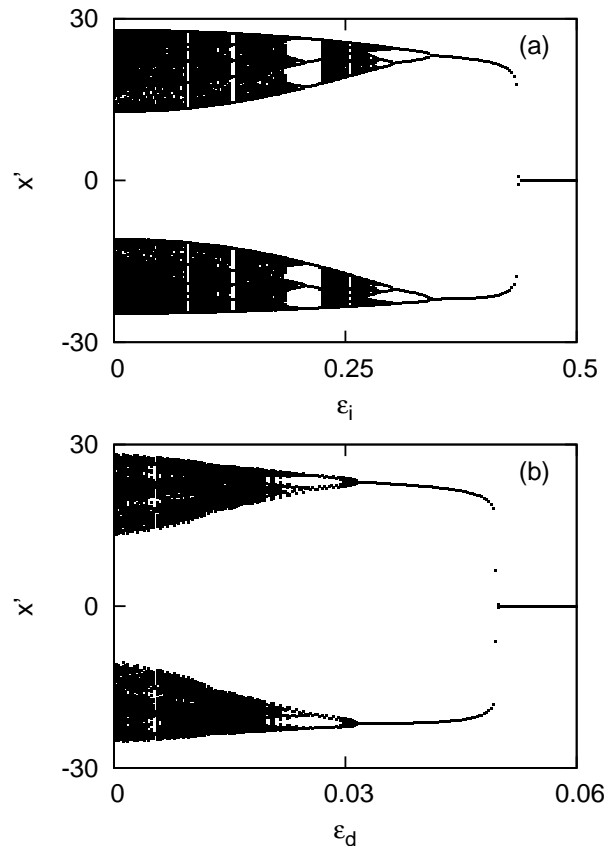


FIG. 7: Bifurcation diagram showing transition to state of amplitude death for coupled Rössler systems. Here, the local maxima and minima (x') of one of the oscillators is plotted against coupling strength. (a) varying ϵ_i while keeping $\epsilon_d = 0.2$ (b) varying ϵ_d while keeping $\epsilon_i = 0.5$.

state, the attractor in the phase space is highly distorted (Fig. 10) and the system is going through a state of frustration, trying to stabilize to antisynchronized state from the synchronized state before death occurs.

The nature of transition to AD is shown in Fig. 11 We see that here, unlike the case of coupled Rössler systems, the amplitude of oscillations drop suddenly at a critical strength of coupling. Here, the transition is directly from chaotic state to AD state. This is again similar to the case of delay coupled Lorenz systems reported in Ref. [24].

5. DISCUSSION

We have shown that indirect coupling through a dynamic environment in addition to direct coupling can lead to amplitude death in chaotic systems, Rössler and Lorenz. They illustrate two typical types of transitions from synchronized state to amplitude death state. We apply the scheme given in 1 to periodic systems such as Landau-Stuart oscillators [14] and van der Pol oscillators as well. We observe amplitude death in both the cases.

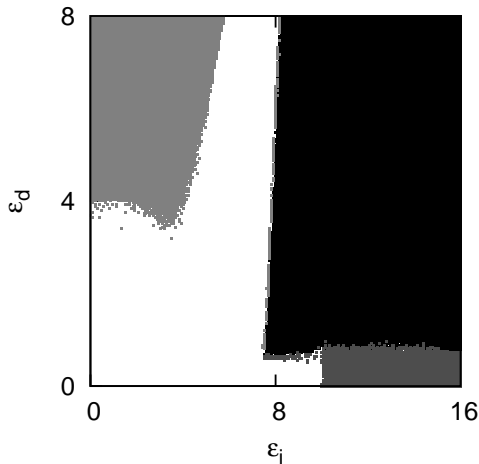


FIG. 8: Regions of different dynamical states in the parameter plane of coupling strengths ($\epsilon_i - \epsilon_d$) in the case of Lorenz systems. Black region corresponds to states of amplitude death ($A \sim 0$), light grey region corresponds to synchronized states ($C \sim 1$), dark grey region correspond to anti-synchronized states ($C \sim -1$) and white region correspond to desynchronized states.

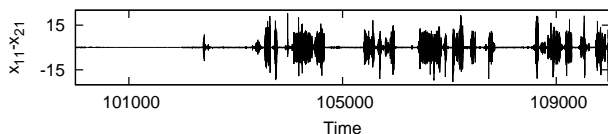


FIG. 9: Synchronization error ($x_{11} - x_{21}$) in the case of Lorenz systems for $\epsilon_d = 5$ and $\epsilon_i = 4.665$.

The details of amplitude death observed in these models are given in Appendix. A. The scheme is also applied to two coupled Mackey-Glass time delay systems [23]. The details of AD in this case is given in Appendix. B.

Our scheme is effective in causing AD in coupled systems where the type of coupling is different from diffusive or linear difference. We have checked this for the cases of Lorenz systems coupled using replacement coupling and synaptically coupled neurons. The replacement coupling leads to synchronization in Lorenz systems as reported in Ref. [22]. We find that for suitable value of coupling strength ϵ_i , the systems stabilize to a state of amplitude death. The details are given in Appendix. D. We also find that this mechanism of amplitude death works in synaptically coupled neuron models such as Hindmarsh-Rose, Hodgkin-Huxley and FitzHugh-Nagumo systems and is useful in explaining the disruption of neuronal activity in the case of Alzheimer's disease. Using numerical studies on these neuronal models, we have shown that the competing effects of synaptic activity and the indirect interaction mediated by a protein $A\beta$ leads to sub-threshold activity and synaptic silencing [18].

However, in the case of driven systems such as driven van der Pol and driven duffing, we find that a stable

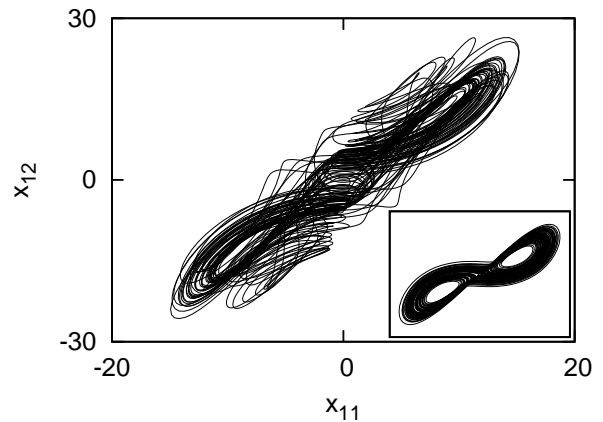


FIG. 10: Phase space diagram of one of the two coupled Lorenz systems given in Eq. 3 for coupling strengths $\epsilon_d = 5.0$ and $\epsilon_i = 7.2$. Phase space diagram of one of the uncoupled Lorenz systems is given in the inset for comparison.

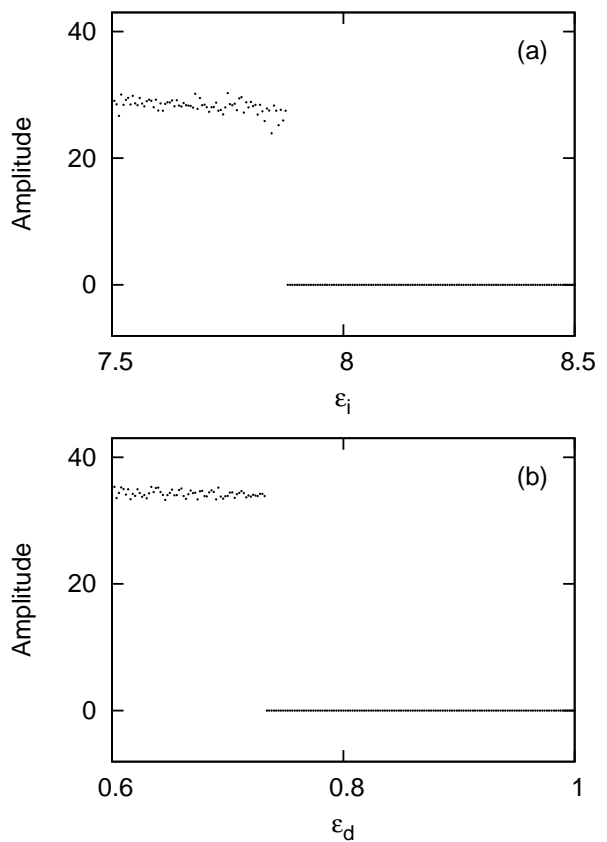


FIG. 11: Transition to state of amplitude death for coupled Lorenz systems. Here, the strength of one coupling is kept fixed, while varying the other. (a) varying ϵ_i while keeping $\epsilon_d = 5.0$ (b) varying ϵ_d while keeping $\epsilon_i = 12.0$. In both cases, the transitions are sudden.

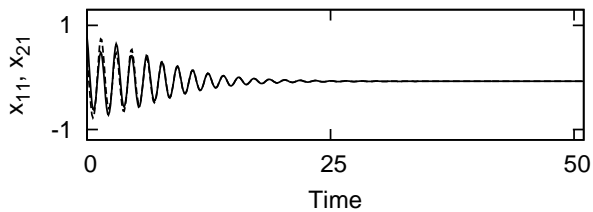


FIG. 12: Time series of the variable x_{i1} of the coupled Landau-Stuart system $(\epsilon_d, \epsilon_i) = (0.5, 3.5)$ showing AD. Here, the transients are not neglected. We take $\omega = 2$ for both the systems.

steady state is not possible and in such cases, small oscillations are observed due to the competing effects of direct and indirect couplings. The details are given in Appendix. C.

In conclusion, the mechanism for amplitude death introduced in this paper is quite general and works for different types of systems such as periodic, chaotic and time-delay systems and also for different types of direct coupling such as diffusive, substitution coupling and synaptic coupling.

Appendix A: Amplitude death in periodic systems

We study two standard limit cycle oscillators, namely Landau-Stuart oscillators and van der Pol oscillators, coupled using the scheme given in Eq. 1. Landau-Stuart system is a nonlinear limit cycle oscillator, which has been previously used as a model system for studying the phenomenon of Amplitude death [13, 14]. In our case, the dynamics of two coupled Landau-Stuart systems is given by the following set of equations.

$$\begin{aligned} \dot{x}_{i1} &= (x_{i1}^2 + x_{i2}^2)x_{i1} - \omega x_{i2} + \epsilon_d(x_{j1} - x_{i1}) + \epsilon_i y \\ \dot{x}_{i2} &= (x_{i1}^2 + x_{i2}^2)x_{i2} + \omega x_{i1} \\ \dot{y} &= -\kappa y - \frac{\epsilon_i}{2} \sum_i x_{i1} \end{aligned} \quad (\text{A1})$$

From numerical analysis of the above equations, we see that, when $\epsilon_i = 0$, and for suitable value of ϵ_d , the systems synchronize. By increasing ϵ_i , the systems can be taken to a state of AD. Time series for the amplitude death states are shown in Fig. 12. We note that, here the transition to the state of amplitude death is sudden, similar to the case of Lorenz systems. This is shown in Fig. 13. However, in this case, for a given strength of coupling, the stability of AD state depends on the initial conditions indicating multi-stability. Such a multi-stability has also been reported for amplitude death phenomena in the case of Landau Stuart oscillators [13].

In Fig. 14 basin of amplitude death is shown for a chosen value of ϵ_i and for varying ϵ_d . White regions represent the basin for amplitude death and black regions represent the basin for oscillatory states. Fig. 14(a), shows

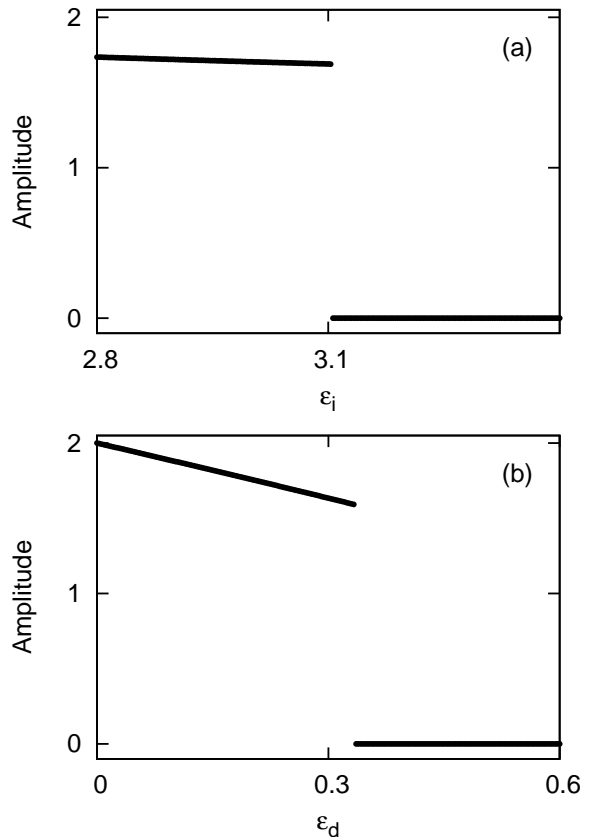


FIG. 13: Transition to amplitude death state in the case of two coupled Landau-Stuart oscillators. (a) fixing $\epsilon_d = 0.5$ and changing ϵ_i (b) fixing $\epsilon_i = 3.5$ and changing ϵ_d

the basin of amplitude death when $\epsilon_d = 0$. Here, AD occurs even in the absence of direct coupling. A possible explanation is that the μ of the individual system is negative or zero such that, the stability condition $\kappa > \mu$ given in Eq. 10 is always satisfied. It is seen that the area of the basin of amplitude death increases as ϵ_d increases (Fig. 14(b)&(c)).

The same analysis is repeated for the case of two coupled periodic van der Pol systems given by the following equations

$$\begin{aligned} \dot{x}_{i1} &= x_{i2} + \epsilon_d(x_{j1} - x_{i1}) + \epsilon_i y \\ \dot{x}_{i2} &= \alpha(1 - x_{i1}^2)x_{i2} - x_{i1} \\ \dot{y} &= -\kappa y - \frac{\epsilon_i}{2} \sum_i x_{i1} \end{aligned} \quad (\text{A2})$$

We choose the parameter α such that the system has a stable limit cycle when both the couplings are absent (i.e., $\epsilon_i = \epsilon_d = 0$). For suitable strength of direct coupling ϵ_d , the systems synchronize and amplitude death is observed when both direct and indirect couplings are above their respective thresholds (Fig. 15). In the case of van der Pol systems, we find that two types of transitions to death occurs. Fixing ϵ_d and increasing ϵ_i , we

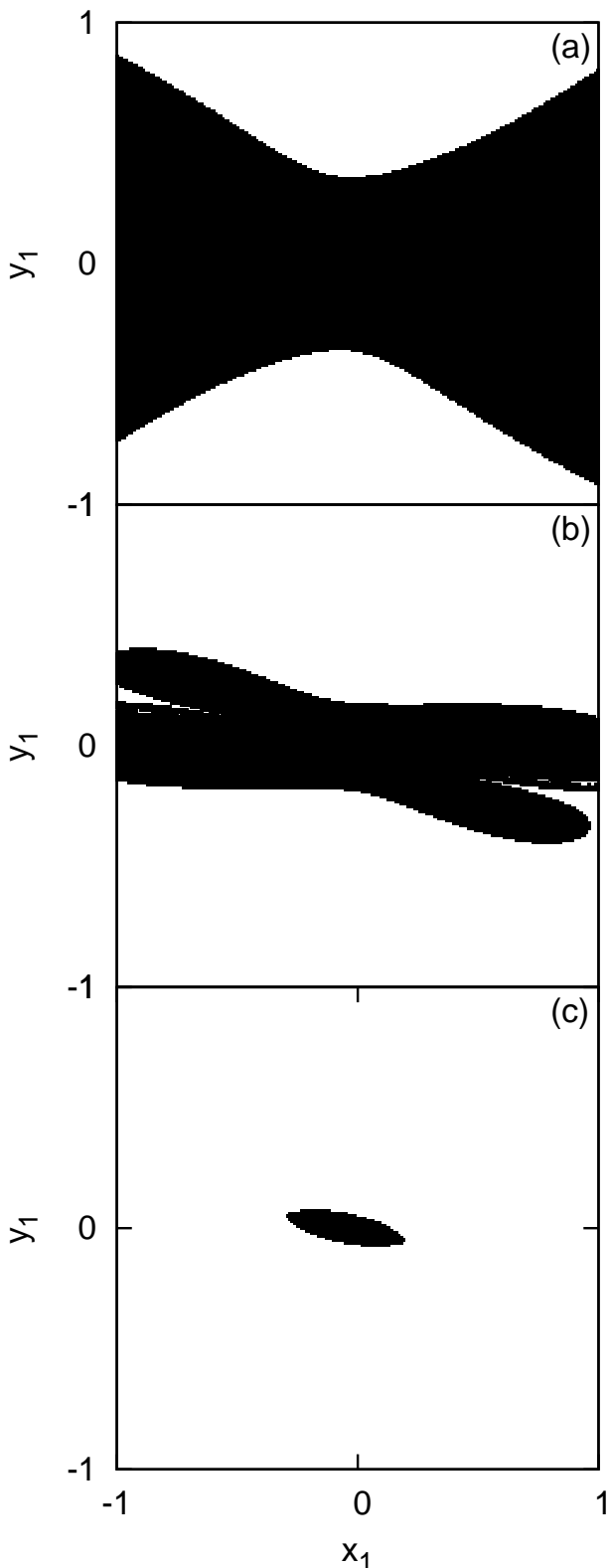


FIG. 14: The basin for amplitude death in the initial conditions (x_1, y_1) of one of the two coupled Landau-Stuart systems. The initial condition of the other system is chosen to be $x_2 = x_1 + 0.1$, $y_2 = y_1$. White regions indicate basin of attraction for amplitude death state, where $A = 0$, and black regions indicate basin for oscillatory state ($A > 0$). The strength of indirect coupling is chosen to be $\epsilon_i = 3.8$, and the strength of direct coupling is varied as (a) $\epsilon_d = 0$ (b) $\epsilon_d = 0.2$ (c) $\epsilon_d = 0.4$. We see that the basin of amplitude death increases as ϵ_d increases.

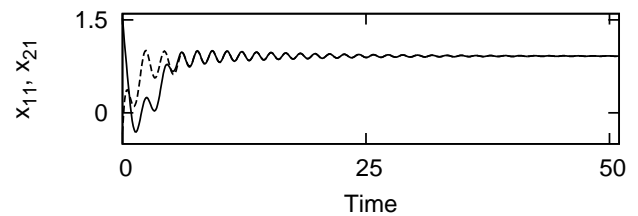


FIG. 15: Time series of the variable x_{i1} of the coupled van der Pol systems for $(\epsilon_d, \epsilon_i) = (1.5, 2.5)$ in AD. Here, the parameter μ for the individual systems are chosen to be $\alpha = 1$ such that the individual systems are in periodic state.

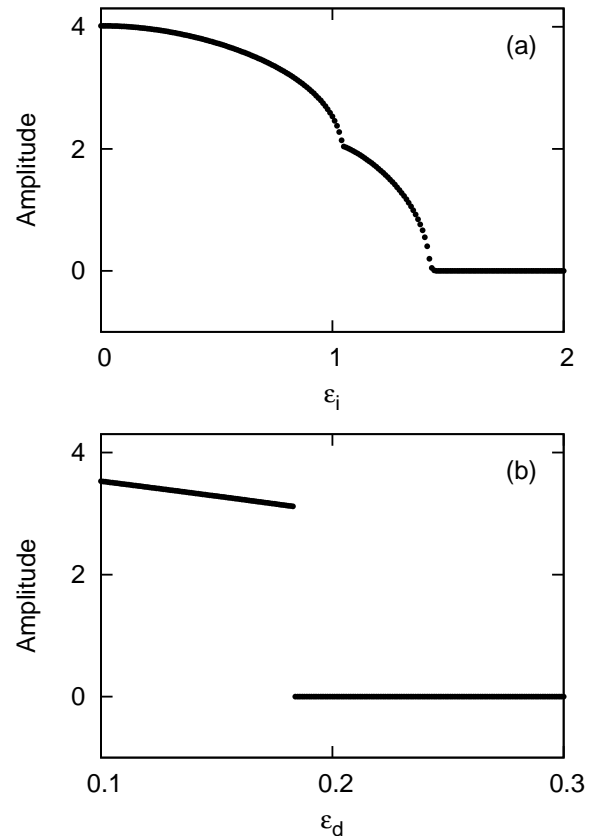


FIG. 16: Transition to amplitude death state in the case of two coupled van der Pol oscillators. (a) fixing $\epsilon_d = 1.5$ and changing ϵ_i (b) fixing $\epsilon_i = 2.0$ and changing ϵ_d

see a smooth transition similar to the case of Rössler systems (Fig. 16 (a)) and by fixing ϵ_i and varying ϵ_d , we get a sudden transition, similar to the case of Lorenz systems (Fig. 16(b)).

Appendix B: Amplitude death in time delay systems

The Mackey Glass time delay system, first introduced as a model for blood generation in patients with leukemia, is well studied as a model exhibiting hyper

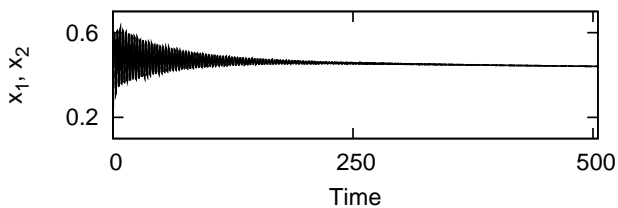


FIG. 17: . Time series of two coupled Mackey-Glass systems showing amplitude death for $(\epsilon_d, \epsilon_i) = (1.5, 1.0)$. For numerical analysis, we have taken the following parameter values to be $\alpha = 1$, $\beta = 2$, $\tau = 2.5, m = 10$, and $\kappa = 1$.

chaos. Here we consider two Mackey-Glass systems coupled via both direct and indirect coupling as given by

$$\begin{aligned} \dot{x}_i &= -\alpha x_i + \frac{\beta x_{\tau i}}{1 + x_{\tau i}^m} + \epsilon_d(x_j - x_i) + \epsilon_i y \\ \dot{y} &= -\kappa y - \frac{\epsilon_i}{2} \sum_{j=1,2} x_j \end{aligned} \quad (\text{B1})$$

where $x_{1,2}$ represents the Mackey-Glass system [23]. When $\epsilon_i = 0$, for sufficiently large coupling strength ϵ_d , the systems synchronize. By increasing ϵ_i we get amplitude death (Fig. 17).

We find that the transition in this case is continuous and that the systems go through a reverse period doubling sequence reaching a limit cycle before amplitude death occurs. This is similar to the case of Rössler systems discussed earlier.

Appendix C: Small oscillations in driven systems

We apply the scheme described in this paper to driven systems such as driven van der Pol and Duffing systems. In such driven systems, steady state does not exist for the individual systems. When these systems are coupled using the both direct and indirect coupling, we observe a regime of small oscillations instead of amplitude death.

The driven van der Pol systems with direct diffusive coupling and indirect coupling through environment can be written as

$$\begin{aligned} \dot{x}_{i1} &= x_{i2} + \epsilon_d(x_{j1} - x_{i1}) + \epsilon_i y \\ \dot{x}_{i2} &= \alpha(1 - x_{i1}^2)x_{i2} - x_{i1} + \beta \cos(\omega t) \\ \dot{y} &= -\kappa y - \frac{\epsilon_i}{2} \sum_j x_{j1} \end{aligned} \quad (\text{C1})$$

We find that, when $\epsilon_i = 0$, and ϵ_d is sufficiently large, we observe synchronization. When ϵ_i is increased, the systems stabilize to a state of small oscillations (Fig. 18).

The same study is repeated for the case of two coupled

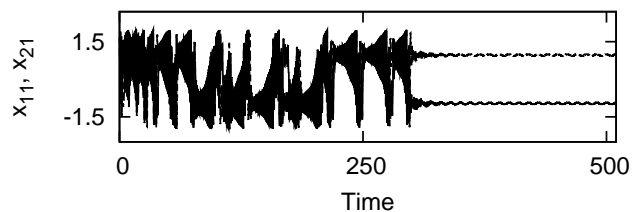


FIG. 18: Time series of the first variable x_{i1} of the coupled driven van der Pol system showing small oscillations for $(\epsilon_d, \epsilon_i) = (1.0, 4.0)$. The parameters of individual systems are taken to be $\alpha = 8.53$, $\omega = 0.2\pi$ and $\beta = 1.2$

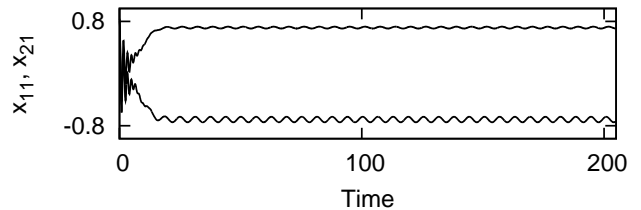


FIG. 19: Time series of the first variable x_{i1} of the coupled driven Duffing system showing small oscillations for $(\epsilon_d, \epsilon_i) = (1.0, 4.0)$. The parameters of individual systems are taken to be $\alpha = 0.25$, $\omega = 1\pi$ and $\beta = 0.3$

Duffing systems given by the following equations

$$\begin{aligned} \dot{x}_{i1} &= x_{i2} + \epsilon_d(x_{j1} - x_{i1}) + \epsilon_i y \\ \dot{x}_{i2} &= -\alpha x_{i2} + x_{i1} - x_{i1}^3 + \beta \cos(\omega t) \\ \dot{y} &= -\kappa y - \frac{\epsilon_i}{2} \sum_j x_{j1} \end{aligned} \quad (\text{C2})$$

We find that a regime of small oscillations is possible in this case also. This is shown in Fig. 2

Appendix D: AD in Lorenz system with replacement coupling

Lorenz systems coupled using a different scheme of coupling, namely replacement coupling, as given by the following equations

$$\begin{aligned} \dot{x}_{i1} &= \sigma(x_{j2} - x_{i1}) + \epsilon_i y \\ \dot{x}_{i2} &= (r - x_{i3})x_{i1} - x_{i2} \\ \dot{x}_{i3} &= x_{i1}x_{i2} - bx_{i3} \\ \dot{y} &= -\kappa y - \frac{\epsilon_i}{2} \sum_i x_{i1} \end{aligned} \quad (\text{D1})$$

Here, the direct coupling is of the replacement type, such that the x_2 variable in the first function of the first system is that of the second system and vice versa. This type of coupling leads to synchronization as reported in [22]. Now, we introduce indirect coupling through variable x_{i1} . We find that for suitable value of coupling

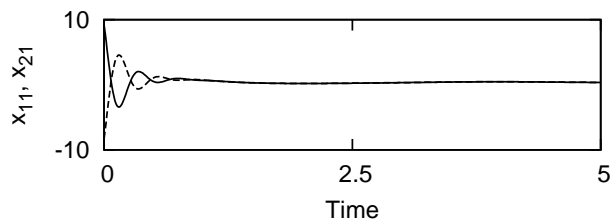


FIG. 20: Time series of the variable x_{i1} of the coupled Lorenz systems where the direct coupling is of substitution type (see text) showing amplitude death for $\epsilon_i = 16.0$.

strength ϵ_i , the systems stabilize to a state of amplitude death. This is shown in Fig. 20

-
- [1] A. S. Pikovsky, M. G. Rosenblum, and J. Kurths, *Synchronization: A Universal Concept in Nonlinear Sciences*, Cambridge Nonlinear Science Series, (Cambridge University Press, London, 2003).
- [2] K. Kaneko, *Theory and Applications of Coupled Map Lattices* (Wiley, New York, 1993).
- [3] E. Ott, *Chaos in Dynamical Systems* (Cambridge University Press, Cambridge, 1993).
- [4] M. Dolnik and M. Marek, *J. Phys. Chem.* **92**, 2452 (1988).
- [5] M. F. Crowley and I. R. Epstein, *J. Phys. Chem.* **93**, 2496 (1989)
- [6] R. Herrero, M. Figueras, J. Rius, F. Pi, and G. Orriols, *Phys. Rev. Lett* **84**, 5312 (2000)
- [7] M. Wei and J. Lun, *Appl. Phys. Lett.* **91**, 061121 (2007).
- [8] D. J. Selkoe, *Ann. N. Y. Acad. Sci.* **924**, 17 (2000).
- [9] R. E. Tanzi, *Nat Neurosci.* **8** 977 (2005).
- [10] B. Caughey, P.T. Lansbury Jr., *Annu. Rev. Neurosci.* **26**, 267 (2003).
- [11] R. E. Mirollo and S. H. Strogatz, *J. Stat. Phys.* **60**, 245 (1990).
- [12] B. Ermentrout, *Physica D* **41**, 219 (1990).
- [13] R. Karnatak, R. Ramaswamy and A. Prasad, *Phys. Rev. E* **76**, 035201 (2007).
- [14] D. V. Ramana Reddy, A. Sen, and G. L. Johnston, *Phys. Rev. Lett.* **80**, 5109 (1998)
- [15] F. M. Atay, *Phys. Rev. Lett.* **91**, 094101 (2003)
- [16] V. Resmi, G. Ambika, and R. E. Amritkar, *Phys. Rev. E* **81**, 046216 (2010).
- [17] A. Wolf, J. B. Swift, H. L. Swinney, and J. A. Vastano, *Physica D* **16**, 285 (1985).
- [18] V. Resmi, G. Ambika, R. E. Amritkar and G. Rangarajan, arXiv:1011.4143v1
- [19] J. Benford, H. Sze, W. Woo, R. R. Smith, and B. Harteneck, *Phys. Rev. Lett.* **62**, 969 (1989)
- [20] M. Y. Kim, R. Roy, J. L. Aron, T. W. Carr, and I. B. Schwartz, *Phys. Rev. Lett.* **94**, 088101 (2005).
- [21] P. Kumar, A. Prasad, and R. Ghosh, *J. Phys. B* **41**, 135402 (2008)
- [22] J. Güémez and M. A. Matías, *Phys. Rev. E* **52**, R2145 (1995)
- [23] M. C. Mackey, and L. Glass, *Science* **197**, 287 (1977).
- [24] A. Prasad, *Phys. Rev. E* **72**, 056204 (2005).